Modeling and Simulation of the New Type of EMI filter for Integrated Power Electronics Modules

Rydlichowski Piotr[1)] and Bandurski Wojciech[1)]

[1)] Poznań University of Technology, Chair of Multimedia Telecommunications and Microelectronics
ul. Polanka 3, 60-965 Poznań
prydlich@et.put.poznan.pl, bandursk@et.put.poznan.pl

Abstract: *Electromagnetic interference (EMI) at radio frequencies (RF) in compact integrated power electronic converter modules can be suppressed using lossy transmission line low-pass filters. This paper presents results of numerical simulations of the filter structure proposed in [1] together with some modifications. Transfer function, surface current distribution and electromagnetic field distribution are considered. The main application of proposed structures is suppression of RF-EMI interference in power electronic devices. Such interferences are found mainly in integrated high power converters (power densities 13 W/cm^3 and above). Interferences are also caused by electromagnetic coupling between electronic devices during switching and by inductance and capacitance in electronic devices and in module package. With new technologies a need has occurred to design new, small, planar low-pass filters for Integrated Power Electronic modules (IPEMs). Mentioned modules with kilowatt powers and high power densities can be a source of significant RF-EMI interferences. Experimental characteristics are compared with one obtained from proposed analytical modeling. The goal of the following paper is to use a professional full-wave electromagnetic simulator to analyze this type of filters, especially current density for different frequencies, derive transfer function and propose a better analytical model.*

Keywords: EMI, planar filters, IPEM, fullwave simulation

1. INTRODUCTION

The following paper is a continuation of our previous work [2] and it is focused on analysis of prototypes of new planar low-pass filters for Integrated Power Electronics Modules (IPEM's). Considered structures are shown in Fig. 1 (not in scale), Fig. 2, Fig. 3, Fig. 4 and Fig. 5. The main application of the proposed structures is suppression of RF-EMI interference in power electronic devices. Such interferences are found mainly in integrated high power converters (power densities 13 W/cm^3 and above). Spurious interferences are result of switching and electromagnetic coupling between elements and by inductance or capacitance of electronic elements. In previous technologies such filters were fabricated as a part of coaxial cable. However, new devices and technologies require planar, compact fabrication. This requirement results in completely new IPEM filter design. Such modules generate kilowatt powers densities and can generate significant RF-EMI interferences. New filters for radio frequency (RF) modules must satisfy three main prerequisites: 1) because the structure should be small the speed of electromagnetic wave must be reduced to fraction of its free-space velocity value, 2) the structure should be electrically and mechanically able to handle power from 1kW to 10kW at 300V to 500V and 30A, 3) the filter cut-off slope should be as steep as possible (e.g., > 40 dB/decade).

Such requirements pose a problem because new technologies, materials and testing procedures are

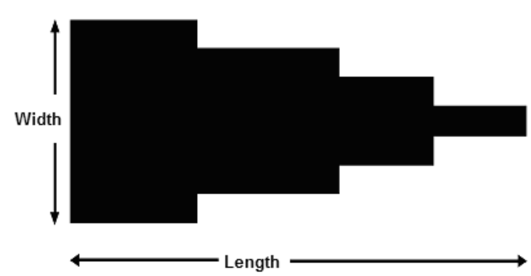

Fig. 1 Plan view of four-section Ni - $BaTiO_3$ - Ni attenuation layer [1]

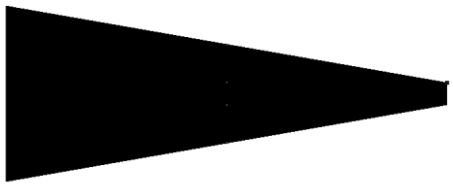

Fig. 2 Plan view of linear Ni - $BaTiO_3$ - Ni attenuation layer

Fig. 3 Plan view of eight-section Ni - $BaTiO_3$ - Ni attenuation layer

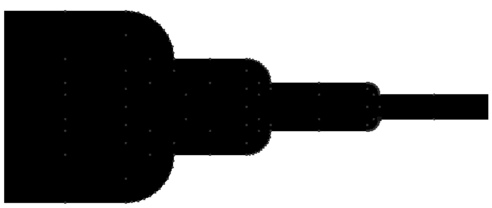

Fig. 4 Plan view of four-section, circularly shaped Ni - $BaTiO_3$ - Ni attenuation layer

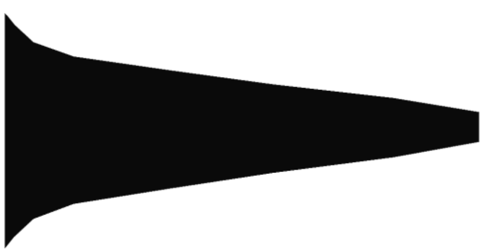

Fig. 5 Plan view of exponentially shaped Ni - $BaTiO_3$ - Ni attenuation layer

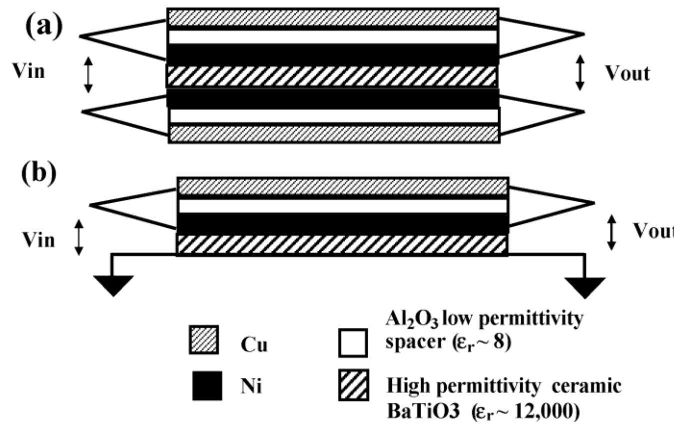

Fig. 6 Cross-section of analyzed filter structures [1]

needed. The prototype structure presented in [1] meets specified above requirements and was already analyzed in previous works [2], [3]. The authors of this paper describe the production technology of this kind of filter and experimental measurements of the transfer function are presented. These characteristics are compared with those obtained from proposed simple analytical modeling [1]. In [3], a better analytical model is proposed and examined. The considered filters have different forward and reverse characteristic, which is caused by geometry (as suggested by authors in [1]) and results in non-uniform current density and EM field distribution in the analyzed structure. This was a topic in the authors' previous work [2]. As mentioned previously, the transfer function is derived in forward and reverse direction. Obtained results - Amplitude characteristics are different from experimental ones, especially in forward direction. Even the better analytical model proposed in [3] does not provide satisfactory results.

The goal of the following paper is to use a professional full-wave electromagnetic simulator to analyze this type of filters, especially current density for different frequencies. Scattering matrix *S* and admittance matrix *Y* for filter transfer function calculation in both forward and reverse direction are used. A new analytical model – transverse resonance technique is proposed. Also filter transfer function modeling technique is proposed which can be useful in further simulations. Conclusions and guidelines for further research work are outlined.

2. Parameters of Analyzed Structures

The proposed filter structure [1] with steps in width was chosen because of simple production and theoretical modeling. Steps are the first approximation of exponential shape. Proposed filter structures are manufactured in form of several layers Cu - Al_2O_3 - Ni -$BaTiO_3$ - Ni - Al_2O_3 - Cu. Filter cross-section is presented on Fig. 6 (without - a and with - b common ground return). The Ni - $BaTiO_3$ - Ni layers are responsible for interferences reduction. Geometry and properties of these layers define filter interference suppression performance. Cu layers carry kW power levels. Unwanted higher order harmonics signals are diverted into Ni – $BaTiO_3$- Ni layers were they are finally suppressed. In [1] the following filter dimensions are assumed: length – 100mm, sections widths – 40mm, 20mm, 10mm and 5mm. Length of each section – 25mm. Thickness: Ni – 17μm, $\sigma = 1{,}47 \cdot 10^7$S/m and $\mu_r = 100$. $BaTiO_3$ layer – 150μm, tan $\Delta = 0.0035\sqrt{(f/10^6)}$ - approximation, $\varepsilon_r = 12000$. The considered simulation frequency range is 1 kHz – 100 MHz. The initial prototype filter structure was characterized by a uniform Ni layer shape. However a non-uniform Ni layer shape is believed to provide higher attenuation levels. $BaTiO_3$ ceramic material is untypical when it comes to filter production and its exact material parameters in different environment conditions are not completely defined, especially thermal properties. These properties also rely heavily on difficult ceramic wafer fabrication process, it is done from powder in sintering process. Presented structures must handle significant power levels and also thermal properties should be considered and most importantly modeled. Figures 2, 3, 4 and show analysed variations of structure on Fig. 1. Every structure is modelled with same 40mm and 5mm terminals width. Structure on Fig. 3 has following sections widths: 40mm, 30mm, 20mm, 15mm, 10mm, 7.5mm, 6.5mm and 5mm. Structure on Fig. 4 has the same sections widths as structure on Fig. 1. Circular edges have 10mm, 5mm and 2.5mm of radius respectively. Structures without sharp edges should be characterized by smaller current crowding effect and higher attenuation.

3. Attenuation Layer Structures Simulation

Full-wave electromagnetic simulations were made using IE3D package from Zeland Corporation. Program uses Method of Moments (MoM) to find discrete form of Maxwell equations. During research work it turned out that one of the most important parameters in presented simulations is meshing frequency. The $BaTiO_3$ ceramic dielectric material has a high ε_r value, causing electric and magnetic field lines to be tightly aligned inside this material. The dielectric parameters define meshing frequency for the whole structure. The high dielectric constant value is responsible for slowing down propagating electromagnetic wave to fraction of its free-space velocity value and consequently shorter wavelength. To obtain accurate results 15-20 mesh cells per wavelength are needed and this results in around 12 GHz meshing frequency for analyzed structures. Numerous simulations have shown that in many cases acceptable accuracy is obtained already at 5 GHz meshing frequency. Higher meshing frequency and finite dielectric modeling guarantee best possible accuracy – more cells in structure are generated but longer simulation times are observed. Research has shown that EM field simulators with accurate 3D dielectric modeling capabilities (most FDTD simulators) are better suited for considered structures than classical MoM simulators (because of high electrical permittivity difference between layers). The optimal program parameters used in simulations must be determined by the user and are a tradeoff between accuracy and simulation time. Structures presented on Fig. 1, Fig. 2, Fig. 3, Fig. 4 and Fig. 5 were simulated in common ground configuration. Ni - $BaTiO_3$ - Ni attenuator structure is untypical because of high dielectric permittivity, which is not found in microstrip microwave filters. Physical and electrical parameters of dielectric material - $BaTiO_3$ are as mentioned earlier unsure and this area requires further research. Recently new kind of material appeared and was proposed, $SrTiO_3$ – it does not show dielectric constant relaxation phenomena. Stepped Ni structure is an first rough approximation of exponential taper and is used because of simple production technology and simplified analytical approach as well. In order to explain Ni - $BaTiO_3$ - Ni attenuation characteristics, current density and electromagnetic field distribution in and around the structure was simulated. Results of

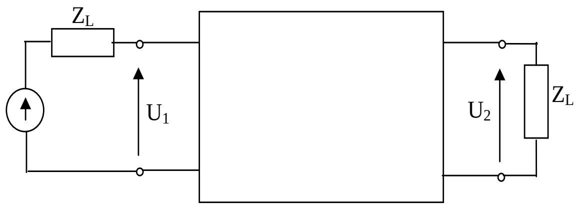

Fig. 7 Filter configuration used in simulations

these simulations can be found in [2]. Because of significant differences in electrical parameters between Ni and $BaTiO_3$ layers, much care must be taken to properly analyze simulation results. In previous works transfer function for each structure was calculated. Structure on Fig. 1 has already been analyzed, was fabricated and exact amplitude characteristic is known [1] and [3]. Filter was simulated in the configuration shown on Fig. 7. We are interested in amplitude characteristic for both forward - $|H_F(\omega)|$ and reverse - $|H_R(\omega)|$ direction. Transfer function $H_F(\omega)$ and $H_R(\omega)$ expressions:

$$H_F(\omega)=\frac{U_2(\omega)}{U_1(\omega)}=\frac{-Y_{21}}{Y_{22}+\frac{1}{Z_L}},H_R(\omega)=\frac{U_1(\omega)}{U_2(\omega)}=\frac{-Y_{12}}{Y_{11}+\frac{1}{Z_L}}. \tag{1}$$

and amplitude characteristics (in dB) are given by:

$$A_F=20\log|H_F(\omega)|,\ A_R=20\log|H_R(\omega)|. \tag{2}$$

Similar procedure can be applied using *S* parameters. Both parameters *Y* and *S* were obtained in series of numerical simulations.

4. Simulations Results For Ni-BaTiO$_3$-Ni Attenuation Layer

The first step was to simulate and analyze current density distribution for structures presented on Fig. 1 – Fig. 5. For lower frequencies 1 kHz – in pass-band we can observe current crowding effect. For higher frequencies, 100MHz we can observe skin depth effect and differences in current density for forward and backward directions. Fig. 8 presents experimental transfer function and best theoretical model obtained by authors in [1] for basic structure from Fig. 1. Detailed results with graphs for current distribution can be found in [2]. Fig. 9 presents amplitude characteristics calculated from *Y* matrix elements (from numerical simulations) for structures on Fig. 1 – Fig. 5. *FH/BH* mean forward and backward direction characteristic. Suffixes *s*, *l*, *x2*, *c* and *x* describe structures from Fig. 1 – Fig. 5 respectively. Detailed simulation results and conclusions were also already presented by the authors in previous work [2].

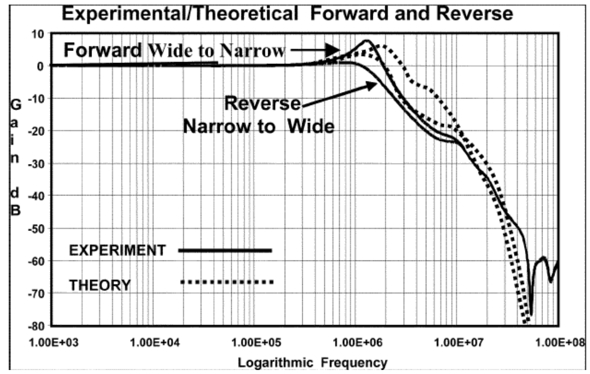

Fig. 8 Experimental and theoretical amplitude characteristics [1]

5. Analytical Modeling

Initially authors in [3] used simple current crowding model to achieve a more accurate transfer function when compared to experimental results. However this analytical model was still not adequate for the transfer function in forward direction. In the following paper, two analytical models are considered. The first one incorporates a transverse resonance technique. This technique allows to derive propagation constants for each layer. The whole structure is treated as a transmission line. Transverse resonance technique is not accurate for structure with more than 5 layers due to multiple reflections. For the simple case of three layers Ni - $BaTiO_3$ – Ni we have the following equations:

$$\gamma_1^2+\gamma_z^2=-\omega^2\mu_1\cdot\varepsilon_1 \qquad \gamma_2^2+\gamma_z^2=-\omega^2\mu_2\cdot\varepsilon_2 \qquad \gamma_{00}^2+\gamma_z^2=-\omega^2\mu_{00}\cdot\varepsilon_{00}$$

$$Z_{c1}=\frac{\gamma_1}{j\cdot\omega\cdot\varepsilon_1} \qquad Z_{c2}=\frac{\gamma_2}{j\cdot\omega\cdot\varepsilon_2} \qquad Z_{c0}=\frac{\gamma_{00}}{j\cdot\omega\cdot\varepsilon_{00}} \tag{3}$$

where γ_1, γ_2 and γ_{00} are the individual propagation constants for each layer and γ_z is the overall propagation constant along the structure. Z_c are characteristic impedances of each layer. Using given above equations final equation for γ_z can be derived:

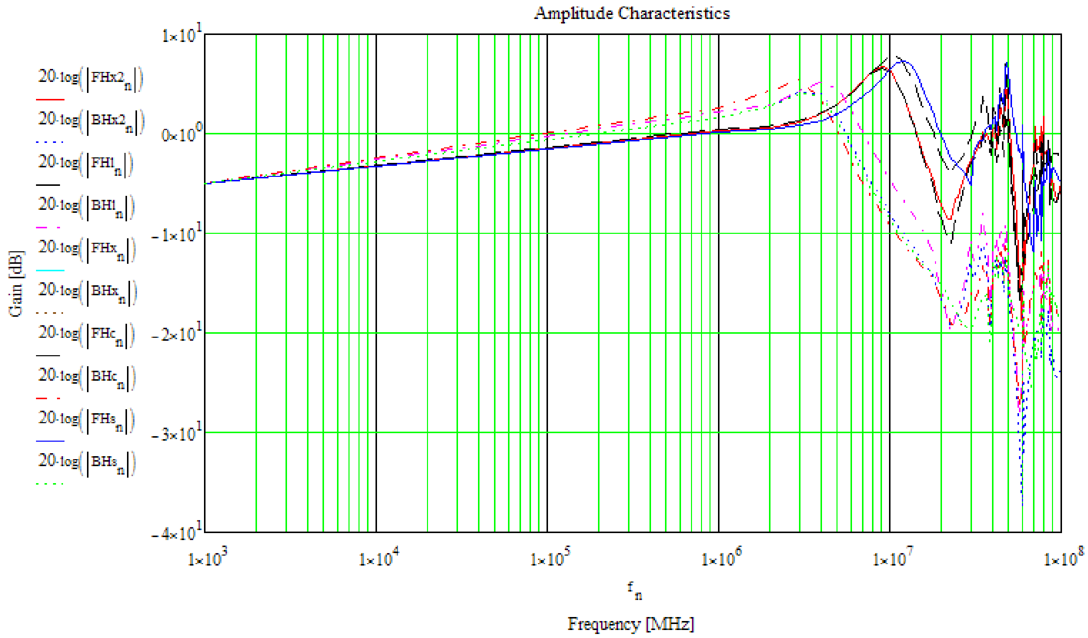

Fig. 9 Ni-$BaTiO_3$-Ni attenuation structures amplitude characteristic

$$Z_{c1}\cdot\frac{Z_{c1}\cdot\tanh(\gamma_1\cdot d_1)+\dfrac{Z_{c0}}{\tanh\left(\dfrac{\gamma_{00}\cdot d_0}{2}\right)}}{Z_{c1}+Z_{c0}\cdot\dfrac{\tanh(\gamma_1\cdot d_1)}{\tanh\left(\dfrac{\gamma_{00}\cdot d_0}{2}\right)}}=-Z_{c2}\cdot\tanh(\gamma_2\cdot d_2) \tag{4}$$

Obtained system of equations for considered structure cannot be solved analytically and further research in this area is required – especially numerical techniques. However if we use the following assumptions:

$$\tanh(\gamma_1\cdot d_1)=\gamma_1\cdot d_1 \qquad \tanh\left(\frac{\gamma_{00}\cdot d_0}{2}\right)=\frac{\gamma_{00}\cdot d_0}{2} \qquad \tanh(\gamma_2\cdot d_2)=\gamma_2\cdot d_2 \tag{5}$$

system can be solved and we obtain the equations for propagation constants. However further analysis have shown that assumption (5) is not true with considered material parameters. Further research work is needed to find a different and more appropriate approximation of hyperbolic tangent function. With such approximation it will be possible to solve equation (4) analytically. Another research direction is to try solve (4) numerically, unfortunately this area has not been studied yet. Initial attempts have shown that because of complex variables in equation numerical solution could be difficult to find.

Accurate analytical transfer function solution would allows us to simulate considered filters in SPICE circuit programs without the need to use time demanding numerical simulations.

Second aspect of analytical approach is to find and synthesize equivalent circuit for each segment and for each step change in width. Such combined equivalent circuit can be modeled in SPICE software. Equivalent circuit parameters can be found using parameter extraction from numerical simulation results. However simulations have shown that for given frequency range it is impossible to find compact/sensible equivalent circuit. Wideband equivalent circuit extraction is required but generated circuit is complicated and difficult to analyze, this is another point of further research.

Currently research is being done to find analytical solutions for transfer function using only numerical data from experimental measurements. Initial results are promising and will be main point of interest in next publication.

6. CONCLUSIONS

The presented simulation results, together with previous publications, prove the expected physical effects in the considered layered structure – current crowding and skin depth. The derived transfer function for the base structure is different from the experimental one, especially in forward direction. Presented analytical models reduced difference between theory and experimental measurements. However, still considerable differences for transfer function in forward direction can be observed. Further research when it comes to modeling considered filter structure in full-wave simulator is required. A better analytical model with accurate wideband parameter extraction is required. The transverse resonance technique requires approximations which would allow to solve propagation constants analytically. Another interesting area is numerical simulations of filter structure with different dielectric materials and with new variations of attenuator structure shape.

REFERENCES

[1] Colin Kydd Campbell, Jacobus Daniel van Wyk, Pieter Wolmarans, *Improved Transmission – Line Attenuators for Integrated Power Filters in the RF Band*, IEEE TRANSACTIONS ON COMPONENTS AND PACKAGING, VOL. 27, NO. 2, JUNE 2004

[2] Piotr Rydlichowski, Wojciech Bandurski, *Modeling of a new planarlowpass filter for Integrated Power ElectronicsModules in IE3D simulator,* 18th INTERNATIONAL WROCLAW SYMPOSIUM AND EXHIBITION ON ELECTROMAGNETIC COMPATIBILITY, WROCLAW, 28 – 30 JUNE, 2006.

[3] Colin Kydd Campbell, Jacobus Daniel van Wyk, Rengang Chen, Effect of Current Crowding on Frequency Response of a Stepped Planar RF Transmission-Line Lowpass Filter for Power Electronics, IEEE TRANSACTIONS ON COMPONENTS AND PACKAGING, VOL. 29, NO. 4, NOVEMBER 2006.